

Fourier Transform Infrared Emission Spectroscopy of the $[6.7]^2\Sigma^+ - X^2\Sigma^+$ System of HfN

R. S. Ram and P. F. Bernath¹

Department of Chemistry, University of Arizona, Tucson, Arizona 85721

Received March 11, 1997; in revised form May 20, 1997

The electronic emission spectrum of HfN has been observed in the near infrared using a Fourier transform spectrometer. HfN molecules were excited in a hafnium hollow cathode lamp operated with neon gas and a trace of nitrogen. The bands located near 5746, 5802, 6668, and 6715 cm^{-1} have been assigned as the 0–1, 1–2, 0–0, and 1–1 bands of the $[6.7]^2\Sigma^+ - X^2\Sigma^+$ transition. The rotational analysis of these bands has been performed and the equilibrium molecular constants for the lower electronic state of ^{180}HfN are $\omega_e = 932.7164(15) \text{ cm}^{-1}$, $\omega_e x_e = 4.41299(65) \text{ cm}^{-1}$, $B_e = 0.436217(18) \text{ cm}^{-1}$, $\alpha_e = 0.002659(11) \text{ cm}^{-1}$, and $r_e = 1.724678(36) \text{ \AA}$. We believe that the lower state of this transition is the ground electronic state but more experimental and theoretical work is necessary to prove this. Our work represents the first experimental observation of an electronic transition of HfN. © 1997 Academic Press

INTRODUCTION

Transition-metal-containing molecules are of theoretical (1–4) and chemical (5–7) importance and their study provides important information needed for the characterization of catalytic processes (6, 7). The spectroscopic study of these molecules also provides insight into chemical bonding in simple metal-containing systems. Transition metal nitrides may also be of astrophysical importance since many transition metal elements have been detected in atomic and molecular form (oxides and hydrides) in the atmospheres of cool M- and S-type stars (8–13). The study of simple transition metal nitrides might give information on the abundance of nitrogen in the atmospheres of cool stars. Experimental data on transition metal nitrides are also necessary to test ab initio calculations and to encourage theoreticians to carry out new calculations. Only a very limited number of ab initio calculations are available for transition metal nitrides.

In recent years considerable progress has been made in the experimental and theoretical studies of transition metal nitrides and several new nitride molecules such as ScN (14), YN (15), WN (16), ReN (17), RhN (18), PtN (19, 20), IrN (21), and CrN (22) have been discovered. Theoretical calculations for ScN (23), YN (24), TiN (25–27), VN (27, 28), and CrN (27) have also been reported. In the IVB transition metal nitride family, the electronic spectra of TiN (29–36) and ZrN (37–40) are known but no reliable information is available for HfN. TiN and ZrN have $^2\Sigma^+$ ground states in agreement with theoretical calculations (for TiN). The infrared spectra of TiN, ZrN, and HfN have been stud-

ied by DeVore *et al.* (41) but their results for TiN and ZrN have proved to be erroneous and the HfN results are also in doubt.

In general, the electronic spectra of transition metal nitrides, particularly in the visible region, are expected to be very complex because of a high density of states complicated by high spin multiplicities and large spin–orbit intervals. These problems are the result of the large number of unpaired d electrons. Many of the electronic states and spin components interact with each other causing extensive perturbations. The infrared electronic transitions of transition metal nitrides are expected to be relatively simple because of the smaller density of states at lower energies.

In the present paper we report on the discovery of an infrared transition of HfN recorded by high-resolution Fourier transform emission spectroscopy. As expected, this $^2\Sigma^+ - ^2\Sigma^+$ transition is free from local perturbations. The lower state of this transition is most probably the ground state of HfN, although more experimental data or some theoretical calculations are needed to make a definite assignment. The excited $^2\Sigma^+$ state probably arises from a low-lying configuration and is analogous to the low-lying $A^1\Sigma^+$ state in ScN (14). The $A^1\Sigma^+ - X^1\Sigma^+$ transition of ScN near 5820 cm^{-1} thus corresponds to the $[6.7]^2\Sigma^+ - X^2\Sigma^+$ transition of HfN.

EXPERIMENTAL

HfN was made in a hafnium hollow cathode lamp which was prepared by inserting a 1-mm-thick cylindrical foil of hafnium metal into a $\frac{1}{4}$ " hole in a copper block. The foil was tightly pressed against the inner wall to provide a close and uniform contact between the hafnium metal and the copper

¹ Also at Department of Chemistry, University of Waterloo, Waterloo, Ontario, Canada N2L 3G1.

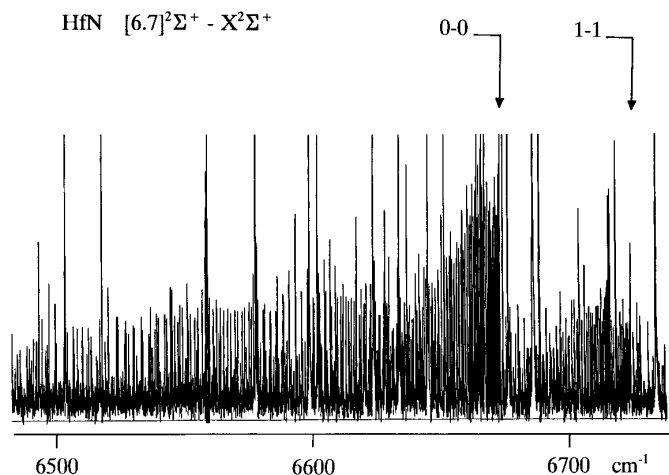


FIG. 1. A compressed portion of the 0-0 and 1-1 bands of HfN.

block. The emission from the lamp was observed with the 1-m Fourier transform spectrometer associated with the McMath–Pierce Solar Telescope of the National Solar Observatory.

Initially we planned to record the HfN transitions in the 10 000–26 000 cm^{-1} interval corresponding to the $A^2\Pi-X^2\Sigma^+$ and $B^2\Sigma^+-X^2\Sigma^+$ transitions of TiN and ZrN. A mixture of 2.5 Torr of Ne and about 6 mTorr of N_2 was discharged with a current at 600 mA at 350 V. Several new bands were observed in the 17 000–26 000 cm^{-1} region with a line spacing appropriate for HfO or HfN. To identify the carrier of these bands, a trace of O_2 was added instead of N_2 . The new bands disappeared entirely and the well-known bands of HfO (42) were seen instead. This experiment suggested that the new bands were due to HfN. Next the 3000–9500 cm^{-1} region was examined and a group of HfN bands appeared in between 5500 and 6800 cm^{-1} . Again the carrier of these bands was confirmed by replacing N_2 with O_2 and noting the appearance of the $b^3\Pi-a^3\Delta$ transition of HfO (43) in the 6900–8000 cm^{-1} region. A partial pressure of about 4 to 6 mTorr of N_2 gave the most suitable HfN spectra since higher pressures of N_2 result in strong N_2 emission.

The spectra from 3500 to 26 000 cm^{-1} were recorded in three parts. The 3500–9200 cm^{-1} spectral region was recorded using InSb detectors and silicon filters with 10 scans co-added in about 70 min of integration. The 10 000–19 000 cm^{-1} region was recorded with red pass filters and silicon diode detectors while the 17 000–26 000 cm^{-1} region was recorded with CuSO_4 filters and silicon diode detectors. The spectrometer resolution was set at 0.02 cm^{-1} in all experiments. The bands in the 17 000–26 000 cm^{-1} region are very complex because of overlapping lines and extensive perturbations. Improved spectra will be recorded in the near future and in this paper we will report only on the infrared bands.

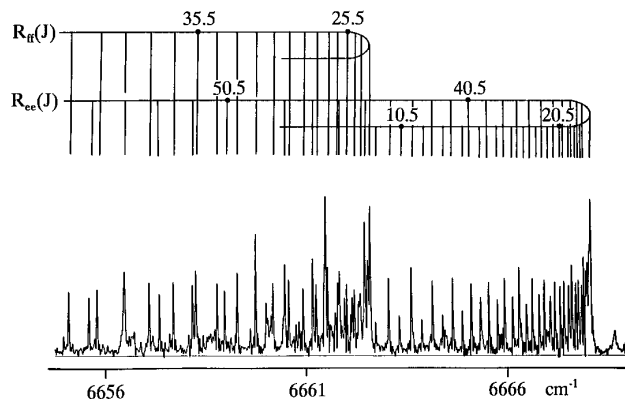


FIG. 2. An expanded portion of the 0-0 band of HfN near the R heads.

In addition to the HfN bands, the observed spectra also contained Hf and Ne atomic lines as well as N_2 molecular lines. The spectra were calibrated using the measurements of Ne atomic lines made by Palmer and Engleman (44). The absolute accuracy of the wavenumber scale is expected to be better than $\pm 0.002 \text{ cm}^{-1}$. The strong lines of HfN appear with a typical signal to noise ratio of 15:1 and have a typical linewidth of about 0.04 cm^{-1} . The precision of measurements of strong and unblended HfN lines is expected to be better than $\pm 0.003 \text{ cm}^{-1}$.

OBSERVATION AND ANALYSIS

The spectral line positions were extracted from the observed spectra using a data reduction program called PC-DECOMP developed by J. Brault. The peak positions were determined by fitting a Voigt lineshape function to each spectral feature. The branches in the different sub-bands were sorted using a color Loomis–Wood program running on a PC computer.

The new infrared bands of HfN are located in the 5500–

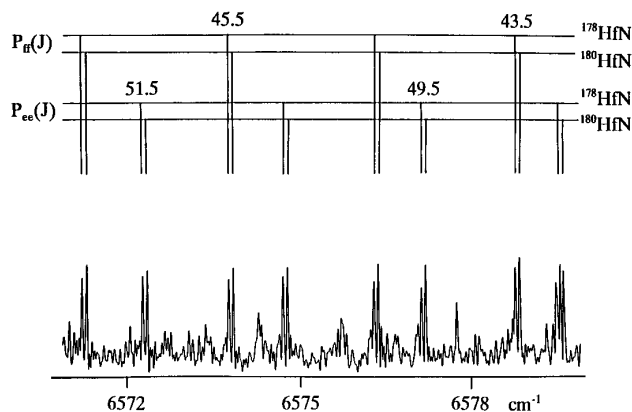


FIG. 3. A portion of the 0-0 band of HfN with some high $J P$ lines of ^{178}HfN and ^{180}HfN marked.

TABLE 1
Observed Wavenumbers (in cm^{-1}) of the $[6.7]^2\Sigma^+ - X^2\Sigma^+$ System of ^{178}HfN

0-0 Band									1-1 Band							
J	Ree	O-C	Pee	O-C	Rff	O-C	Pff	O-C	Ree	O-C	Pee	O-C	Rff	O-C	Pff	O-C
1.5					6656.871	7										
2.5	6657.597	5	6653.249	3	6657.482	-1										
3.5	6658.437	3	6652.427	10	6658.072	6	6650.717	2	6704.237	-14					6696.281	4
4.5	6659.239	-3			6658.621	7	6649.603	11	6705.078	-10	6697.386	8			6695.120	-1
5.5	6660.006	-8	6650.663	8	6659.127	0	6648.448	12	6705.889	0	6696.515	-5			6693.929	1
6.5	6660.756	4	6649.731	8	6659.609	4					6695.626	-1			6692.686	-13
7.5	6661.468	14	6648.760	6	6660.046	-2			6707.382	-3	6694.695	-3			6691.452	16
8.5	6662.123	2	6647.759	8	6660.475	19	6644.765	12	6708.073	-8	6693.732	-2	6705.642	-10	6690.141	3
9.5	6662.754	1	6646.722	9	6660.830	1			6708.735	-4	6692.736	1	6705.968	-7	6688.806	4
10.5	6663.353	3	6645.652	13	6661.176	9			6709.370	6	6691.698	-2	6706.258	-5	6687.436	4
11.5	6663.915	2	6644.540	9	6661.468	-1	6640.766	10	6709.949	-4	6690.632	1	6706.509	-5	6686.039	13
12.5	6664.441	1	6643.401	12	6661.741	5			6710.499	-8	6689.529	4	6706.725	-5	6684.590	6
13.5	6664.934	1			6661.972	3	6637.928	11	6711.020	-4	6688.390	5	6706.905	-4	6683.117	10
14.5	6665.393	3	6641.008	8	6662.166	-1	6636.442	-4	6711.506	-1	6687.216	6	6707.050	-3	6681.616	22
15.5	6665.815	2			6662.328	-1	6634.929	-11	6711.948	-6	6686.002	3	6707.154	-7		
16.5	6666.202	0	6638.464	-8			6633.392	-6	6712.359	-7	6684.761	8	6707.227	-5	6678.473	12
17.5	6666.555	0							6712.736	-7	6683.476	3	6707.268	0	6676.864	23
18.5	6666.872	-2	6635.813	7	6662.618	12	6630.209	-3	6713.080	-5			6707.268	0	6675.200	14
19.5	6667.157	0	6634.417	-3			6628.571	5	6713.386	-4	6680.814	7	6707.227	-4		
20.5	6667.406	0	6632.995	-6			6626.882	-4	6713.655	-6			6707.154	-5		
21.5	6667.619	-1	6631.541	-7	6662.558	-11	6625.167	-5	6713.894	-4	6678.007	6	6707.050	-1	6670.030	25
22.5	6667.798	-2	6630.054	-5	6662.482	-4	6623.418	-4	6714.093	-5	6676.553	8	6706.905	-1	6668.226	19
23.5	6667.944	-1	6628.527	-10	6662.371	2	6621.635	-4	6714.261	-2	6675.067	11	6706.725	0	6666.368	-5
24.5	6668.047	-9	6626.972	-8	6662.218	1	6619.816	-5	6714.389	-5	6673.532	1	6706.509	1	6664.494	-9
25.5	6668.135	4	6625.385	-5	6662.029	-1	6617.968	-1	6714.486	-3	6671.992	20	6706.258	3		
26.5	6668.172	0	6623.759	-6	6661.806	-3	6616.082	0	6714.549	-1	6670.396	19	6705.968	3		
27.5			6622.102	-4	6661.554	2	6614.155	-5			6668.771	23	6705.642	3		
28.5			6620.408	-6	6661.261	0	6612.201	-4	6714.566	1	6667.097	12	6705.281	3		
29.5	6668.085	-6	6618.682	-5	6660.934	-1	6610.214	-2	6714.516	-4	6665.393	6	6704.884	5	6654.605	-14
30.5	6667.995	0	6616.917	-9	6660.575	0	6608.190	-2	6714.433	-7	6663.656	1	6704.448	3	6652.538	3
31.5	6667.862	-2	6615.129	-3	6660.179	-1	6606.129	-5	6714.324	-1	6661.904	17	6703.975	1	6650.413	-3
32.5	6667.699	-2	6613.299	-4	6659.747	-4	6604.041	-1	6714.172	-4			6703.468	2	6648.258	-1
33.5	6667.500	-2	6611.439	-3	6659.287	0	6601.916	0	6713.988	-3	6658.255	4	6702.923	1	6646.063	-5
34.5	6667.267	-2	6609.541	-5	6658.788	-1	6599.757	1	6713.769	-3	6656.379	-2	6702.337	-4	6643.846	5
35.5	6667.002	-1			6658.255	0	6597.563	0	6713.515	-2	6654.476	-1	6701.723	-1	6641.580	2
36.5	6666.700	-3	6605.653	-3	6657.689	1	6595.340	5	6713.225	-3	6652.538	-1	6701.071	0	6639.292	13
37.5	6666.368	-1	6603.659	-1	6657.087	0	6593.071	-3	6712.902	-2	6650.562	-4	6700.382	2	6636.945	0
38.5	6665.998	-2	6601.629	-2	6656.467	15	6590.777	-2	6712.541	-4	6648.561	2	6699.653	0	6634.576	2
39.5	6665.597	-2	6599.567	-2	6655.782	1	6588.447	-3	6712.150	-2	6646.519	1	6698.889	0	6632.159	-8
40.5	6665.161	-2	6597.473	-1	6655.077	0	6586.088	0	6711.725	1	6644.445	2	6698.094	5	6629.731	5
41.5	6664.693	-1	6595.340	-6	6654.340	1	6583.690	-3	6711.258	-3			6697.251	-1	6627.253	7
42.5	6664.189	-2	6593.182	-3	6653.569	2			6710.760	-3	6640.197	5	6696.377	0	6624.731	-2
43.5	6663.656	0	6590.990	-1	6652.761	0	6578.799	-3	6710.230	-2	6638.018	3	6695.468	2	6622.187	5
44.5	6663.083	-3	6588.756	-9	6651.923	3	6576.304	-2	6709.664	-1	6635.813	9	6694.509	-9	6619.595	-1
45.5	6662.482	-1	6586.506	1	6651.048	1	6573.774	-4	6709.064	2	6633.566	6	6693.542	9	6616.968	-4
46.5	6661.847	-1	6584.213	0	6650.143	4	6571.211	-5	6708.427	0	6631.285	4	6692.510	0	6614.301	-13
47.5	6661.176	-3	6581.884	-5	6649.203	5	6568.617	-5	6707.756	-1	6628.974	5	6691.452	1	6611.622	4
48.5	6660.475	-1	6579.536	3	6648.226	3	6565.990	-4	6707.050	-1	6626.619	-4	6690.358	4	6608.890	3
49.5	6659.747	5	6577.144	0	6647.231	17	6563.335	1	6706.309	-2	6624.247	3	6689.223	3	6606.129	10
50.5	6658.975	1	6574.721	-2	6646.177	5	6560.639	-2	6705.536	-1	6621.824	-6	6688.055	7	6603.303	-13
51.5	6658.174	1	6572.268	-3	6645.105	8	6557.909	-7	6704.728	-1	6619.390	7	6686.846	7		
52.5	6657.342	2	6569.786	0	6643.993	5	6555.157	-1	6703.883	-2	6616.917	15	6685.593	1	6597.617	20
53.5	6656.467	-8	6567.266	-3	6642.855	9	6552.363	-4	6703.006	-1	6614.390	1	6684.318	11	6594.682	-2
54.5	6655.578	2	6564.718	-2			6549.540	-4	6702.095	1	6611.829	-12	6682.993	8	6591.728	-6
55.5	6654.651	5	6562.139	-2	6640.453	-10	6546.682	-6	6701.148	0	6609.262	2	6681.616	-8	6588.756	8
56.5	6653.686	3	6559.530	1	6639.213	-8	6543.800	-2	6700.167	0	6606.643	-3			6585.723	0
57.5	6652.693	5	6556.885	-1	6637.928	-19	6540.881	-1	6699.150	0	6603.994	-3	6678.773	-17	6582.659	-4
58.5	6651.664	3	6554.216	3	6636.623	-17	6537.931	0	6698.094	-7	6601.319	3				
59.5	6650.608	7	6551.505	-2	6635.292	-9	6534.942	-5	6697.012	-4	6598.596	-5	6675.793	-9	6576.433	2
60.5	6649.517	6	6548.773	2	6633.918	-9	6531.930	-3	6695.900	4	6595.843	-10	6674.250	0	6573.253	-7
61.5	6648.394	5	6546.005	0	6632.519	-4	6528.880	-6	6694.743	0	6593.071	0	6672.656	-4		
62.5	6647.231	-3	6543.207	0	6631.086	0	6525.797	-11	6693.542	-13	6590.253	-3			6566.794	-10
63.5	6646.063	15	6540.379	0	6629.616	0	6522.696	-2	6692.336	4	6587.403	-4	6669.357	-7		
64.5	6644.839	8	6537.523	3	6628.113	0	6519.558	0	6691.074	-1	6584.523	-2			6560.201	2
65.5	6643.591	9	6534.636	5	6626.579	0	6516.391	6	6689.781	-2			6665.905	-6	6556.839	-1

Note. O-C are observed minus calculated line positions in units of 10^{-3}cm^{-1} .

TABLE 1—Continued

0-0 Band									1-1 Band							
J	Ree	O-C	Pee	O-C	Rff	O-C	Pff	O-C	Ree	O-C	Pee	O-C	Rff	O-C	Pff	O-C
66.5			6531.712	0	6625.011	-1	6513.181	-1	6688.452	-3	6578.661	0	6664.133	8	6553.452	9
67.5	6641.008	15	6528.760	-2	6623.418	4	6509.949	1	6687.101	7	6575.677	-2			6550.006	-1
68.5	6639.664	13			6621.777	-7	6506.680	-4	6685.701	2	6672.657	-7	6660.435	0	6546.535	0
69.5	6638.292	13	6522.771	-3	6620.118	-4	6503.388	0	6684.273	5	6569.612	-3	6658.527	-3	6543.021	-2
70.5	6636.894	18	6519.735	-1	6618.429	1	6500.063	1	6682.809	7	6566.519	-14	6656.584	-2	6539.470	-3
71.5	6635.465	22	6516.668	0	6616.706	4	6496.703	-3	6681.315	12	6563.420	3	6654.605	5	6535.885	0
72.5	6634.002	23			6614.948	3	6493.316	-2			6560.264	-4	6652.581	7	6532.270	12
73.5			6510.446	2	6613.161	3	6489.905	4	6678.196	-2	6557.082	-3	6650.511	3	6528.579	-13
74.5			6507.288	0	6611.342	4	6486.450	-3	6676.604	12	6553.869	0	6648.394	-7	6524.874	-13
75.5	6629.402	-5	6504.102	-1	6609.491	4	6482.980	4	6674.970	18	6550.616	-3	6646.239	-14		
76.5	6627.820	-2	6500.895	5	6607.613	7	6479.468	-1			6547.327	-9	6644.049	-14		
77.5	6626.206	-3	6497.650	2	6605.703	9	6475.930	-2	6671.567	0	6544.023	3				
78.5	6624.554	-12	6494.382	4	6603.752	2	6472.368	3	6669.823	1	6540.667	-2				
79.5			6491.077	-2	6601.775	-1	6468.769	-1	6668.047	5	6537.283	-1				
80.5	6621.184	-7	6487.759	7	6599.757	-15	6465.150	6	6666.202	-24	6533.863	-3				
81.5	6619.450	-10	6484.399	2	6597.738	0	6461.497	8	6664.389	15	6530.417	3				
82.5	6617.707	6	6481.020	5	6595.677	5	6457.811	5	6662.482	-4						
83.5	6615.905	-7	6477.607	2	6593.583	6	6454.094	0	6660.575	11	6523.409	0				
84.5	6614.084	-10	6474.171	3	6591.458	6	6450.364	11			6519.853	-2				
85.5	6612.251	2	6470.702	-1	6589.305	9	6446.582	-2			6516.270	3				
86.5	6610.372	-3			6587.117	5	6442.787	2			6512.637	-6				
87.5	6608.469	-3	6463.691	-1	6584.902	5	6438.969	10								
88.5	6606.539	-3	6460.148	1	6582.659	6	6435.105	0								
89.5	6604.579	-5	6456.573	-2	6580.378	-2	6431.227	5			6501.563	-7				
90.5	6602.599	0	6452.965	-12	6578.081	4					6497.784	-25				
91.5			6449.343	-9	6575.733	-13	6423.363	-11								
92.5	6598.542	-3	6445.706	4	6573.370	-15	6419.413	6								
93.5			6442.028	2	6570.995	-1										
94.5	6594.377	-5	6438.344	20	6568.573	-5	6411.388	-6								
95.5	6592.259	-2	6434.595	-1												
96.5	6590.103	-10	6430.844	0			6403.263	-10								
97.5	6587.941	3	6427.065	-1	6561.143	-10										
98.5					6558.615	-7										
99.5			6419.446	9	6556.048	-15										

0-1 Band									1-2 Band							
J	Ree	O-C	Pee	O-C	Rff	O-C	Pff	O-C	Ree	O-C	Pee	O-C	Rff	O-C	Pff	O-C
3.5					5733.843	-13										
4.5					5734.427	-4					5781.993	-10				
5.5					5734.968	-8	5724.292	8			5781.161	-11				
6.5	5736.595	-6					5723.131	1			5780.316	6				
7.5	5737.350	9			5735.975	-3	5721.938	-7	5792.101	-5	5779.412	-6				
8.5	5738.049	-2	5723.684	3	5736.421	-13	5720.728	-3	5792.842	-1	5778.493	-4	5790.465	4		
9.5	5738.738	7	5722.696	5					5793.542	-9	5777.545	-1	5790.822	-15	5773.670	5
10.5	5739.387	4	5721.671	0	5737.243	-14	5718.211	-2	5794.225	-3	5776.564	0	5791.188	5	5772.342	-10
11.5	5740.025	21	5720.622	0	5737.622	-2	5716.913	3	5794.878	3	5775.555	3	5791.496	-2	5771.007	-3
12.5	5740.591	-4	5719.516	-28	5737.943	-17	5715.580	2	5795.504	12	5774.510	-1	5791.786	4	5769.638	1
13.5	5741.143	-15	5718.431	-5	5738.273	5	5714.205	-11			5773.436	-4	5792.044	8	5768.238	4
14.5	5741.692	1	5717.300	1	5738.539	-6	5712.826	1	5796.625	-10	5772.342	4	5792.265	6	5766.805	5
15.5	5742.192	-2	5716.131	-2	5738.790	-4	5711.400	-4	5797.160	-2	5771.204	-3	5792.454	3	5765.335	-1
16.5	5742.659	-9	5714.941	4	5739.023	11	5709.959	6	5797.660	1			5792.616	3	5763.844	2
17.5	5743.109	-3	5713.714	1	5739.205	4	5708.474	-1	5798.129	4					5762.321	4
18.5	5743.535	8	5712.457	-2	5739.387	27	5706.965	0	5798.562	-1	5767.631	-5	5792.842	-2	5760.759	-3
19.5	5743.900	-13	5711.182	6			5705.433	6	5798.973	4	5766.387	2			5759.181	4
20.5	5744.275	7	5709.859	-5			5703.872	12			5765.101	-5	5792.956	4	5757.567	7
21.5	5744.592	-4	5708.522	0					5799.694	1	5763.795	-1			5755.920	5
22.5	5744.889	-4	5707.141	-12			5700.635	-3			5762.460	2			5754.243	5
23.5	5745.146	-15	5705.751	-3					5800.296	-2	5761.091	2	5792.892	8	5752.531	0
24.5	5745.404	3	5704.324	-2	5739.701	7	5697.318	20	5800.558	3	5759.692	0	5792.805	6	5750.795	1
25.5	5745.617	7	5702.872	3	5739.652	5	5695.569	-17	5800.785	2	5758.267	2	5792.674	-9	5749.030	5

TABLE 1—Continued

0-1 Band									1-2 Band							
J	Ree	O-C	Pee	O-C	Rff	O-C	Pff	O-C	Ree	O-C	Pee	O-C	Rff	O-C	Pff	O-C
26.5	5745.795	3	5701.374	-10	5739.575	5	5693.846	2	5800.987	6	5756.811	3	5792.518	-18	5747.233	5
27.5	5745.938	-6	5699.880	10	5739.479	15	5692.070	-2			5755.324	1	5792.354	-5	5745.404	5
28.5	5746.068	2	5698.324	-3	5739.337	8	5690.287	15	5801.284	-3	5753.809	2	5792.141	-9	5743.535	-5
29.5	5746.160	-1	5696.757	1	5739.161	-2	5688.457	13			5752.265	2	5791.909	-1	5741.651	1
30.5			5695.159	3			5686.586	0			5750.693	3	5791.639	0	5739.743	13
31.5			5693.528	0	5738.738	-8	5684.705	5			5749.084	-2			5737.778	-2
32.5			5691.871	-1	5738.491	-3	5682.782	-3			5747.457	2	5791.002	-2	5735.803	4
33.5			5690.182	-5	5738.221	9	5680.846	4	5801.542	8	5745.795	1	5790.643	3		
34.5	5746.195	-3	5688.457	-18	5737.896	-6	5678.873	3	5801.492	-2	5744.100	-4	5790.245	0	5731.748	3
35.5	5746.112	-7	5686.733	-1	5737.565	3	5676.870	1			5742.386	1	5789.816	-3	5729.671	-2
36.5	5746.016	4			5737.177	-17	5674.842	2	5801.332	5	5740.642	4	5789.362	2	5727.585	16
37.5	5745.886	10	5683.164	-4	5736.798	2	5672.771	-12	5801.200	2	5738.868	7	5788.869	-3	5725.436	0
38.5	5745.710	-3	5681.344	1	5736.359	-10	5670.690	-8	5801.039	-2	5737.059	4	5788.341	-10	5723.265	-7
39.5	5745.522	2	5679.492	2			5668.584	1	5800.853	0	5735.220	0	5787.794	-5	5721.074	-3
40.5	5745.302	3	5677.611	1	5735.439	8	5666.438	-4	5800.644	7	5733.357	0	5787.211	-4	5718.846	-5
41.5	5745.055	4	5675.705	3	5734.915	-3	5664.270	-2			5731.469	4	5786.597	-3	5716.593	-2
42.5	5744.776	2	5673.767	0	5734.375	-2			5800.115	-1	5729.545	1	5785.945	-8	5714.310	2
43.5	5744.460	-9	5671.806	1	5733.799	-9	5659.844	-4	5799.822	10	5727.585	-10	5785.269	-5	5711.994	4
44.5	5744.143	7	5669.815	0	5733.210	1	5657.601	6	5799.468	-10	5725.620	2	5784.560	-5	5709.650	8
45.5	5743.762	-13	5667.795	-2	5732.577	-6	5655.317	3	5799.119	5	5723.611	-1	5783.817	-6		
46.5	5743.388	1	5665.747	-6	5731.923	-5	5653.007	2	5798.728	6	5721.580	4	5783.048	-1		
47.5	5742.971	0	5663.682	0	5731.238	-6	5650.675	7	5798.302	1	5719.516	3	5782.240	-4		
48.5	5742.524	-3	5661.579	-4	5730.533	0	5648.306	2	5797.852	3	5717.424	3	5781.402	-4	5699.934	-5
49.5	5742.056	1	5659.457	-1	5729.789	-5	5645.919	5	5797.370	2	5715.300	-1	5780.534	-2	5697.431	-5
50.5	5741.560	4	5657.303	-3	5729.022	-4	5643.494	-1	5796.857	-3	5713.158	5	5779.629	-5	5694.898	-4
51.5	5741.032	1	5655.130	2	5728.231	0	5641.049	0	5796.324	4	5710.977	1	5778.697	-3	5692.332	-4
52.5	5740.468	-9	5652.922	-1	5727.403	-4	5638.570	-6	5795.749	-4	5708.774	3	5777.732	-2	5689.738	-3
53.5			5650.675	-16	5726.555	0	5636.077	1	5795.146	-10	5706.536	-1	5776.734	-1	5687.107	-6
54.5			5648.434	0	5725.672	-4	5633.548	-1	5794.529	0	5704.271	-5	5775.697	-7	5684.451	-2
55.5	5738.647	-8	5646.148	-2	5724.767	-2	5630.997	2	5793.871	-2	5701.985	0	5774.632	-8	5681.762	-1
56.5	5737.995	1	5643.844	4	5723.846	12	5628.419	4	5793.197	8	5699.671	3	5773.540	-4	5679.041	0
57.5	5737.301	-5	5641.501	-3	5722.873	0	5625.806	-2			5697.318	-3	5772.417	3	5676.290	2
58.5	5736.595	4	5639.137	-6	5721.885	2	5623.178	3	5791.735	4	5694.949	2	5771.252	0	5673.503	1
59.5	5735.858	8			5720.861	-6			5790.954	-6	5692.544	-1	5770.053	-4	5670.690	4
60.5	5735.083	0			5719.821	-2	5617.828	0			5690.115	1	5768.838	9	5667.841	4
61.5	5734.285	-3	5631.905	1	5718.755	3	5615.114	-2			5687.657	2	5767.565	-1	5664.953	-3
62.5	5733.462	-6	5629.442	1	5717.648	-6	5612.381	4					5766.269	-3		
63.5	5732.625	3	5626.955	3	5716.527	-2	5609.615	3	5787.574	-4	5682.652	-2	5764.944	2	5659.101	2
64.5	5731.748	-1	5624.444	6	5715.377	0	5606.813	-9	5786.657	-3	5680.111	-1	5763.587	7	5656.126	3
65.5	5730.859	7	5621.902	2	5714.205	7	5604.004	-1	5785.711	-2	5677.546	6	5762.185	2		
66.5	5729.947	20	5619.340	3	5712.993	0	5601.169	6	5784.736	0	5674.941	-1	5760.759	6		
67.5	5728.981	2	5616.751	2	5711.758	-3	5598.294	-2	5783.729	-2	5672.313	-2	5759.295	7	5647.010	13
68.5	5727.999	-5	5614.137	1	5710.497	-6	5595.406	4	5782.696	1	5669.650	-10	5757.793	3	5643.894	5
69.5	5727.011	7	5611.487	-12			5592.488	3	5781.632	2	5666.970	-7			5640.755	6
70.5	5725.977	-1	5608.837	-1	5707.902	-5	5589.546	5	5780.534	-2	5664.270	4	5754.690	3	5637.588	12
71.5	5724.937	10	5606.150	-3	5706.583	13	5586.568	-5	5779.412	0	5661.528	1	5753.093	9	5634.379	10
72.5	5723.846	-6	5603.447	4	5705.221	14	5583.583	3	5778.254	-6	5658.760	0	5751.448	2	5631.133	4
73.5	5722.751	-1	5600.712	1	5703.834	16	5580.567	6			5655.966	1	5749.772	-1	5627.853	-3
74.5	5721.627	0	5597.955	1			5577.516	-3	5775.863	-2	5653.137	-5	5748.061	-2	5624.547	-1
75.5			5595.176	2	5700.955	-7	5574.448	-3	5774.632	9	5650.288	-2	5746.310	-8	5621.209	2
76.5			5592.369	-1	5699.500	4	5571.361	2	5773.366	14	5647.418	7			5617.828	-4
77.5	5718.098	-7	5589.547	3	5698.008	4	5568.244	1	5772.047	-4	5644.508	6			5614.415	-7
78.5			5586.699	5	5696.489	2	5565.108	6	5770.723	3	5641.561	-6				
79.5	5715.630	-7	5583.827	5	5694.949	3	5561.937	-1								
80.5	5714.365	-1	5580.927	0	5693.373	-4	5558.746	-4			5635.616	7				
81.5	5713.064	-9			5691.785	-1	5555.535	-2			5632.584	-4				
82.5	5711.758	4									5629.536	-2				
83.5											5626.465	5				
84.5											5623.347	-6				
85.5											5620.215	-2				
86.5											5617.053	0				
87.5											5613.856	-4				
88.5											5610.637	0				
89.5											5607.384	-2				

6800 cm^{-1} region. The spectrum consists of four double-headed bands with the higher wavenumber heads at 5746, 5802, 6668, and 6715 cm^{-1} . Inspection of these bands at high resolution indicates that each band consists of four branches, two *R*-type and two *P*-type. The lines of the bands with high wavenumber heads at 6668 and 6715 cm^{-1} do not show any additional doubling at low *J* but the high *J* lines become broad and are split into two components with increasing *J* values. In the bands with the high wavenumber heads at 5746 and 5802 cm^{-1} , the splitting is apparent even for the lowest *J* lines. These four bands have been assigned as 0–0, 1–1, 0–1, and 1–2 bands of a single transition and the observed splitting is attributed to isotope structure. A portion of the compressed spectrum of the 0–0 and 1–1 bands is presented in Fig. 1. Figure 2 is an expanded portion of the 0–0 band with some low *J* lines marked. Hafnium has six naturally occurring isotopes ^{174}Hf (0.2%), ^{176}Hf (5.2%), ^{177}Hf (18.6%), ^{178}Hf (27.3%), ^{179}Hf (13.6%), and ^{180}Hf (35.1%). The two sets of lines for each *J* value have been assigned as mainly the ^{178}HfN and ^{180}HfN isotopomers. The ^{178}Hf and ^{180}Hf nuclei are the most abundant and they have zero nuclear spin. The ^{177}Hf (18.6%) and ^{179}Hf (13.6%) isotopes also have significant abundance but they have high nuclear spins of 7/2 and 9/2, respectively. The lines of ^{177}HfN and ^{179}HfN are expected to be split into 8 and 10 hyperfine components which would not be seen in our spectra at the present resolution and signal-to-noise ratio. Some of the high *J* lines of the 0–0 band are presented in Fig. 3 to illustrate the ^{178}HfN and ^{180}HfN isotope splitting. The lines of both ^{178}HfN and ^{180}HfN have been measured and used in separate rotational analyses. The assignment of the rotational lines in different bands was made using the traditional method of comparing the combination differences for the common vibrational levels.

The fit of the observed lines was obtained utilizing the effective Hamiltonian of Brown *et al.* (45). The matrix elements for a ${}^2\Sigma$ Hamiltonian are listed by Douay *et al.* (46). The T_v , B_v , D_v , and γ_v molecular constants were determined for the lower $X^2\Sigma^+$ state, while for the excited $[6.7]^2\Sigma^+$ state the T_v , B_v , D_v , H_v , γ_v , γ_{Dv} , and γ_{Hv} constants were required to obtain a satisfactory fit. The constant H_0 was not determined for the excited state. The rotational lines were given suitable weights depending on signal-to-noise ratio and extent of blending. The line positions of ^{178}HfN and ^{180}HfN are provided in Tables 1 and 2 and the constants obtained for the upper and lower ${}^2\Sigma^+$ states of ^{178}HfN and ^{180}HfN are listed in Tables 3 and 4, respectively. The *e/f* parity of the rotational levels was chosen to give a negative γ constant in the $X^2\Sigma^+$ state of HfN to be consistent with TiN and ZrN.

DISCUSSION

An inspection of the rotational constants of ^{178}HfN and ^{180}HfN (Tables 3 and 4) indicates that the spin–rotation

parameter γ of the excited state is large compared to that in the lower state. This is a reflection of a strong interaction with a nearby ${}^2\Pi$ state. The successful determination of higher order spin–rotation constants, γ_D and γ_H , for the excited state can also be attributed to these interactions. No local rotational perturbations have been found in any of the analyzed bands.

The rotational constants for the individual vibrational levels of ^{178}HfN (Table 3) and ^{180}HfN (Table 4) have been used to evaluate the equilibrium molecular constants for the two states (Table 5). The ground state equilibrium constants for ^{180}HfN [$\omega_e = 932.7164(15) \text{ cm}^{-1}$, $B_e = 0.436217(18) \text{ cm}^{-1}$] can be used in the isotopic relationships (47), $\omega_e^i = \rho\omega$ and $B_e^i = \rho^2 B_e$ with $\rho^2 = [\mu/\mu^i]$, to test for consistency. The calculated values for ^{178}HfN using the equilibrium constants of ^{180}HfN are $\omega_e = 933.0945 \text{ cm}^{-1}$ and $B_e = 0.436576 \text{ cm}^{-1}$ which can be compared with the experimental values of $\omega_e = 933.0978(19) \text{ cm}^{-1}$ and $B_e = 0.436585(15) \text{ cm}^{-1}$ for ^{178}HfN . The excited state equilibrium constants also obey the isotopic relations in a satisfactory manner. The equilibrium rotational constants have been used to evaluate the bond lengths of 1.724678(36) and 1.7600471(57) Å for the lower and upper states of the most abundant ^{180}HfN isotopomer while the corresponding values for ^{178}HfN are 1.724652(28) and 1.7600229(80) Å, respectively. The observed lower state r_e value is similar in magnitude to that of HfO (48) ($r_e = 1.723071 \text{ Å}$). The equilibrium constants for HfN and HfO have the same pattern as the TiN, TiO and ZrN, ZrO pairs of molecules (48).

The possibility that these new bands could arise from HfO was considered, although the experimental and chemical evidence does not support this assignment. The HfO molecule has known electronic states of either singlet or triplet multiplicity. The observation of doubled *R* and *P* branches with a large spin splitting evident at low *N* values does not fit with any of the possible HfO transitions. The observed lines also fit with half integral *J* values inconsistent with singlet or triplet assignments.

The ground states of TiN and ZrN are well established as ${}^2\Sigma^+$ states by experiment and, for TiN, by theoretical calculations (25–27). By analogy we expect a ${}^2\Sigma^+$ ground state for HfN. For TiN and ZrN several excited states are also known. TiN has $A^2\Delta$, $A^2\Pi$, and $B^2\Sigma^+$ states at 7533, 16 238, and 23 576 cm^{-1} above the ground state while the corresponding $A^2\Pi$ and $B^2\Sigma^+$ states of ZrN are located at 17 401 and 24 670 cm^{-1} . The observation of an excited ${}^2\Sigma^+$ state at about 6650 cm^{-1} is not consistent with expectations based on TiN and ZrN. We do not think that the $[6.7]^2\Sigma^+ - X^2\Sigma^+$ transition of HfN is the $B^2\Sigma^+ - X^2\Sigma^+$ transition since the $A^2\Pi - X^2\Sigma^+$ and $B^2\Sigma^+ - X^2\Sigma^+$ transitions should be found in the 17 000–26 000 cm^{-1} region. At this stage, therefore, we are unable to say with certainty that the observed lower state is in fact the ground state of HfN. It is

TABLE 2—Continued

0-0 Band									1-1 Band							
J	Ree	O-C	Pee	O-C	Rff	O-C	Pff	O-C	Ree	O-C	Pee	O-C	Rff	O-C	Pff	O-C
67.5	6641.008	-3	6528.880	7	6623.459	11	6510.075	-1	6687.101	-1	6575.764	-13	6662.328	-5	6550.145	13
68.5	6639.664	-7	6525.910	14	6621.824	6	6506.811	-3	6685.701	-6	6572.764	0	6660.475	5	6546.682	20
69.5	6638.292	-8	6522.891	2	6620.160	3	6503.522	2	6684.273	-4	6569.716	-1			6543.159	5
70.5	6636.894	-3	6519.853	0	6618.469	4	6500.196	-1	6682.809	-4	6566.637	0	6656.633	9	6539.608	0
71.5			6516.788	2	6616.745	3	6496.841	-2	6681.315	1			6654.651	9	6536.022	0
72.5					6614.989	3	6493.459	1			6560.376	-1	6652.632	13	6532.403	4
73.5			6510.570	2	6613.206	7	6490.042	-2	6678.196	-15	6557.184	-13	6650.562	7	6528.760	24
74.5			6507.417	3	6611.389	8	6486.597	-3	6676.604	-3			6648.448	-2	6525.015	-20
75.5					6609.541	9	6483.123	-2	6674.970	2	6550.740	4	6646.296	-8		
76.5			6501.021	0			6479.622	2	6673.306	11	6547.457	1	6644.108	-10	6517.505	-8
77.5			6497.784	2	6605.750	8	6476.085	-1	6671.608	21	6544.148	6	6641.881	-8		
78.5			6494.517	3	6603.802	2	6472.523	0	6669.859	17	6540.794	1			6509.820	-14
79.5			6491.221	3	6601.830	2	6468.927	-2	6668.085	22	6537.426	14	6637.318	11	6505.913	-21
80.5			6487.894	1	6599.815	-9	6465.308	1	6666.252	3	6534.007	10				
81.5	6619.499	5	6484.540	-1	6597.802	10	6461.654	-1	6664.395	-5	6530.549	1				
82.5	6617.739	3	6481.159	-2	6595.736	8	6457.977	3			6527.071	6				
83.5	6615.951	2	6477.755	1	6593.638	3	6454.263	-2			6523.563	14				
84.5			6474.327	8			6450.527	0	6658.622	-15	6520.000	2				
85.5	6612.294	6	6470.862	5												
86.5	6610.420	4	6467.369	2			6442.967	2			6512.816	21				
87.5	6608.511	-4	6463.856	5			6439.142	1								
88.5	6606.586	1	6460.310	2	6582.720	1	6435.294	4								
89.5	6604.632	3			6580.449	1	6431.409	-1								
90.5	6602.644	-1	6453.144	1	6578.152	5	6427.503	0								
91.5			6449.525	4	6575.825	8	6423.558	-10								
92.5	6598.595	2	6445.878	5	6573.457	-1	6419.615	10								
93.5	6596.523	-4	6442.198	-2	6571.078	8										
94.5	6594.429	-5	6438.514	14	6568.647	-7	6411.594	-3								
95.5	6592.306	-8	6434.775	-1	6566.196	-14	6407.548	-5								
96.5	6590.164	-3	6431.025	-1												
97.5	6587.989	-5	6427.249	-2												
98.5			6423.454	3												
99.5					6556.142	-6										
100.5					6553.563	0										

0-1 Band									1-2 Band							
J	Ree	O-C	Pee	O-C	Rff	O-C	Pff	O-C	Ree	O-C	Pee	O-C	Rff	O-C	Pff	O-C
1.5													5787.345	9		
2.5													5783.952	14	5787.933	8
3.5			5728.562	-6	5734.240	8							5783.183	15	5788.485	2
4.5			5727.737	10	5734.811	4	5725.797	3					5782.364	-4	5789.003	-9
5.5			5726.856	0	5735.347	-5	5724.674	5	5790.903	4	5781.539	2	5789.507	-2	5778.988	9
6.5			5725.977	22	5735.858	-9	5723.517	1	5791.693	-4	5780.671	-5	5789.975	-1	5777.786	-3
7.5			5725.018	-7	5736.359	7	5722.321	-11	5792.454	-9	5779.778	-8	5790.417	4	5776.564	-5
8.5			5724.073	8	5736.798	-10			5793.197	-3	5778.857	-8	5790.822	3	5775.326	8
9.5			5723.073	-3	5737.243	9	5719.876	0			5777.912	-2	5791.188	-7	5774.039	2
10.5	5739.743	-12	5722.053	-5	5737.622	-8	5718.600	-4	5794.582	-1			5791.547	6	5772.717	-9
11.5	5740.375	-1	5721.012	2	5737.995	-2	5717.300	-2	5795.233	3	5775.917	-5	5791.858	3	5771.388	4
12.5	5740.974	7	5719.929	-4	5738.327	-7	5715.974	3	5795.844	-2			5792.141	2		
13.5	5741.515	-14	5718.846	20	5738.647	6			5796.439	7	5773.809	-2	5792.397	4	5768.617	6
14.5	5742.056	-5	5717.692	2			5713.218	-2	5796.989	1	5772.717	6	5792.616	0	5767.179	0
15.5	5742.564	0	5716.527	2	5739.161	-5	5711.803	3	5797.509	-6	5771.579	-2	5792.805	-3	5765.717	1
16.5	5743.035	-3			5739.387	3	5710.356	5	5798.008	-3	5770.426	5	5792.956	-13	5764.226	3
17.5	5743.481	-1	5714.105	-2	5739.575	2	5708.872	-1	5798.475	-3	5769.217	-14	5793.102	1	5762.702	3
18.5	5743.900	3	5712.851	-3	5739.743	11			5798.914	0	5768.008	-4	5793.197	-3	5761.148	2
19.5	5744.275	-6	5711.571	-1			5705.829	0	5799.333	12	5766.759	-4			5759.562	1
20.5	5744.638	0	5710.259	-2			5704.271	8	5799.694	-3	5765.478	-6	5793.313	5	5757.948	1
21.5	5744.969	4	5708.923	2			5702.666	-2	5800.046	2	5764.174	-2				
22.5	5745.251	-11	5707.553	1			5701.045	2	5800.351	-10	5762.838	-1			5754.626	-1
23.5	5745.522	-8	5706.156	2			5699.392	3	5800.644	-3	5761.470	-1	5793.247	8	5752.925	3
24.5			5704.714	-14	5740.077	10	5697.706	0	5800.905	0	5760.079	4	5793.152	-3	5751.188	3
25.5	5745.980	1			5740.025	6	5695.996	1	5801.139	7	5758.648	-1	5793.043	4	5749.422	3
26.5	5746.160	0	5701.785	-4	5739.951	8	5694.252	-2	5801.332	2	5757.191	-3	5792.892	-1	5747.628	6

TABLE 2—Continued

J	0-1 Band								1-2 Band							
	Ree	O-C	Pee	O-C	Rff	O-C	Pff	O-C	Ree	O-C	Pee	O-C	Rff	O-C	Pff	O-C
27.5	5746.310	-1	5700.275	-1	5739.843	7	5692.486	1	5801.492	-6	5755.709	0	5792.717	2	5745.795	0
28.5	5746.434	0	5698.734	0	5739.701	0	5690.687	1	5801.634	-2	5754.194	-1	5792.518	11	5743.938	1
29.5	5746.531	3	5697.161	-3	5739.529	-8	5688.873	14			5752.652	0	5792.265	-2	5742.056	7
30.5	5746.576	-17	5695.569	3	5739.337	-6	5687.006	2	5801.831	7	5751.081	1	5791.999	2	5740.130	-1
31.5	5746.624	-5	5693.936	-4	5739.115	-4			5801.883	10	5749.475	-3	5791.693	-3	5738.182	-1
32.5			5692.282	-2	5738.868	1	5683.211	5			5747.847	-1	5791.359	-3		
33.5			5690.597	-4	5738.588	3	5681.253	-10			5746.195	7	5791.002	4	5734.188	-5
34.5			5688.873	-17	5738.273	-2	5679.295	2			5744.504	5	5790.598	-5	5732.155	2
35.5	5746.484	-3	5687.153	3	5737.943	7	5677.292	-2	5801.759	-14	5742.780	-2	5790.174	-3	5730.083	1
36.5	5746.380	1	5685.383	1	5737.565	-3	5675.267	0	5801.678	3	5741.032	-4	5789.721	1		
37.5	5746.251	7	5683.587	0	5737.177	6	5673.209	-2	5801.542	-5	5739.259	-1			5725.848	-1
38.5	5746.068	-12	5681.762	-1	5736.744	0	5671.136	9	5801.386	-3	5737.460	4	5788.710	-1	5723.684	-3
39.5	5745.886	-1	5679.911	-2	5736.292	2	5669.015	0	5801.200	-2	5735.626	3	5788.160	1	5721.494	1
40.5	5745.665	-2	5678.033	-1	5735.803	-3	5666.873	-2	5800.987	1	5733.760	-1	5787.574	-1	5719.267	-2
41.5	5745.404	-15	5676.128	0	5735.294	0	5664.712	5	5800.737	-3	5731.872	1	5786.960	-1	5717.012	-3
42.5	5745.146	5	5674.193	-1	5734.752	-1	5662.509	-1	5800.463	-3	5729.947	-4	5786.315	0	5714.733	4
43.5	5744.840	3	5672.232	0	5734.188	4	5660.284	-3	5800.163	2	5727.999	-5	5785.638	0	5712.412	-2
44.5	5744.504	0	5670.242	-2			5658.037	2	5799.822	-5	5726.040	13	5784.927	-1	5710.066	-2
45.5	5744.143	0	5668.231	3	5732.956	-4	5655.752	-3	5799.468	4	5724.023	1	5784.184	-3	5707.692	2
46.5	5743.762	7			5732.300	-5	5653.457	8	5799.070	-2	5721.994	5	5783.409	-5	5705.278	-4
47.5	5743.339	0	5664.116	2	5731.622	-1	5651.127	13	5798.649	-1	5719.929	1	5782.607	-2	5702.834	-9
48.5	5742.900	5	5662.021	3	5730.912	1	5648.751	0	5798.201	1	5717.838	1	5781.770	-3	5700.372	-1
49.5	5742.432	8	5659.894	0	5730.171	-1	5646.362	0	5797.719	0	5715.720	2	5780.900	-3	5697.867	-5
50.5	5741.926	1	5657.742	-1	5729.405	0	5643.944	-1	5797.210	0	5713.572	0	5780.000	-2	5695.338	-2
51.5	5741.398	-2	5655.567	0	5728.609	-1	5641.501	1	5796.671	-1	5711.400	4	5779.071	1	5692.775	-2
52.5	5740.846	0	5653.363	0	5727.786	0	5639.028	-1	5796.101	-3	5709.192	-1	5778.101	-2	5690.182	-1
53.5	5740.263	-3	5651.127	-6	5726.936	0	5636.531	0	5795.504	-3	5706.965	4	5777.105	-1	5687.555	-2
54.5	5739.652	-6	5648.879	2	5726.040	-17	5634.003	-3	5794.878	-3	5704.714	12	5776.075	-1	5684.900	0
55.5	5739.023	-1	5646.597	2	5725.153	3	5631.454	-1	5794.225	-1			5775.007	-6	5682.212	0
56.5	5738.366	3	5644.289	2	5724.223	7	5628.872	-4	5793.542	0	5700.099	3	5773.916	-2	5679.492	-1
57.5	5737.674	-1	5641.953	1	5723.265	10	5626.258	-12	5792.842	14	5697.752	0	5772.790	1	5676.738	-3
58.5	5736.968	7	5639.600	8	5722.266	0	5623.635	-4	5792.090	5	5695.384	4	5771.629	0	5673.959	0
59.5			5637.208	1	5721.244	-6	5620.981	0			5692.976	-3			5671.136	-9
60.5	5735.439	-14	5634.799	3	5720.206	-1	5618.294	-2	5790.511	-1	5690.553	3			5668.300	1
61.5	5734.660	1	5632.361	2			5615.584	-1	5789.676	-6	5688.096	3	5767.952	6	5665.420	-1
62.5	5733.843	5	5629.893	-4	5718.040	1	5612.847	-1	5788.821	-2	5685.602	-6	5766.659	6	5662.509	-1
63.5	5733.001	9	5627.409	-1	5716.913	-2	5610.084	-2	5787.933	-2	5683.097	2	5765.335	10	5659.570	2
64.5			5624.899	2	5715.765	1	5607.292	-6	5787.017	0	5680.551	-4	5763.973	9	5656.597	2
65.5	5731.238	15	5622.361	0	5714.592	7	5604.478	-6	5786.073	2	5677.986	1	5762.573	4	5653.605	17
66.5	5730.306	6	5619.795	-4	5713.381	0	5601.643	0	5785.093	-1	5675.385	-4	5761.148	7	5650.550	1
67.5	5729.351	0	5617.213	0	5712.151	1	5598.776	-2	5784.092	3	5672.771	7	5759.692	14	5647.479	1
68.5	5728.378	2	5614.611	9	5710.892	0	5595.886	-1	5783.048	-6	5670.115	4	5758.182	2	5644.377	4
69.5			5611.961	-6			5592.968	-3	5781.993	3	5667.431	1	5756.652	3	5641.237	1
70.5	5726.360	8	5609.314	6	5708.298	-1			5780.900	4	5664.712	-9	5755.086	3		
71.5	5725.299	-3	5606.628	4	5706.965	3	5587.063	-1	5779.778	4			5753.482	1	5634.861	-1
72.5	5724.223	-4	5603.917	0	5705.608	8	5584.065	-7	5778.630	9	5659.218	-1	5751.850	4	5631.630	4
73.5	5723.131	3			5704.215	2			5777.438	-1	5656.429	3	5750.172	-3	5628.362	6
74.5	5721.994	-10	5598.440	9	5702.791	-7	5578.016	0	5776.230	1	5653.605	0	5748.467	-1	5625.046	-6
75.5	5720.861	6	5595.657	4	5701.374	15	5574.946	-5	5775.007	19	5650.758	2	5746.717	-8	5621.714	0
76.5	5719.683	1	5592.857	5	5699.880	-15	5571.863	2	5773.718	1	5647.871	-7			5618.343	0
77.5	5718.485	0	5590.024	-4	5698.410	7	5568.745	-3	5772.417	0	5644.977	5	5743.109	-23	5614.925	-12
78.5	5717.259	-5	5587.180	0	5696.888	-1	5565.610	0	5771.086	-1	5642.044	6			5611.487	-9
79.5	5716.014	-4	5584.311	0	5695.338	-9	5562.440	-9			5639.080	4				
80.5	5714.733	-16	5581.413	-5	5693.793	12			5768.337	-1	5636.077	-8				
81.5	5713.452	-5	5578.503	0	5692.201	10			5766.916	-2	5633.067	1				
82.5	5712.151	10	5575.561	-4							5630.020	1				
83.5	5710.801	0	5572.607	2	5688.941	6			5763.973	-15	5626.955	12				
84.5	5709.436	-2	5569.619	-5	5687.277	6			5762.460	-17	5623.840	1				
85.5	5708.056	3			5685.602	20			5760.929	-7	5620.700	-5				
86.5	5706.639	-6	5563.587	-9	5683.877	8					5617.543	0				
87.5			5560.557	7	5682.125	-7					5614.352	0				
88.5					5680.372	2					5611.131	-2				
89.5					5678.581	-4										

TABLE 3
Spectroscopic Constants (in cm^{-1}) for ^{178}HfN

Const. ^a	$X^2\Sigma^+$			$[6.7]^2\Sigma^+$	
	v=0	v=1	v=2	v=0	v=1
T_v	0.0	924.26295(87)	1839.69110(116)	6654.88281(50)	7624.83890(104)
B_v	0.4352586(31)	0.4325814(32)	0.4299346(32)	0.4177434(31)	0.4148042(32)
$10^7 \times D_v$	3.8390(31)	3.8696(45)	3.8633(32)	3.0907(30)	3.6219(45)
$10^{12} \times H_v$	--	0.154(34)	--	--	-3.355(38)
γ_v	-0.05521(28)	-0.05528(28)	-0.05540(28)	0.16864(28)	0.24337(28)
$10^6 \times \gamma_{Dv}$	--	--	--	1.986(12)	6.323(24)
$10^{10} \times \gamma_{Hv}$	--	--	--	0.420(11)	3.548(34)

^aNumbers in parentheses are one standard deviation in last digit.

very unlikely that the $B^2\Sigma^+$ state will be significantly lower in energy in HfN than in TiN and ZrN. An alternate explanation for the new infrared transition may be that the excited state arises from another low-lying configuration.

The $\text{Hf}\equiv\text{N}$ molecule has a nominal triple bond with the unpaired electron located in a nonbonding Hf $6s$ orbital. The valence electronic configuration of the $X^2\Sigma^+$ state is thus $(1\sigma)^2(1\pi)^4(2\sigma)^2(3\sigma)^1$ with nonbonding 1σ molecular orbital having mainly N $2s$ character. Using

the ScN and TiN calculations for guidance we expect that HfN has two strong π bonds due to the 4 electrons in the 1π orbital made up of mainly Hf $5d\pi$ and N $2p\pi$ atomic orbitals. The weak σ bond results from occupation of the 2σ molecular orbital of mainly Hf $5d\sigma$ and N $2p\sigma$ character. The σ bond is easily broken to give a $:\text{Hf}=\text{N}^{\cdot}$ structure with a $(1\sigma)^2(1\pi)^4(2\sigma)^1(3\sigma)^2$ configuration. It is this configuration which gives rise to the $[6.7]^2\Sigma^+$ state. The $[6.7]^2\Sigma^+ - X^2\Sigma^+$ transition of HfN

TABLE 4
Spectroscopic Constants (in cm^{-1}) for ^{180}HfN

Const. ^a	$X^2\Sigma^+$			$[6.7]^2\Sigma^+$	
	v=0	v=1	v=2	v=0	v=1
T_v	0.0	923.89041(65)	1838.95486(93)	6654.88959(42)	7624.46527(83)
B_v	0.4348938(21)	0.4322172(21)	0.4295770(22)	0.4173938(21)	0.4144591(22)
$10^7 \times D_v$	3.8269(22)	3.8431(22)	3.8535(23)	3.0806(21)	3.6155(34)
$10^{12} \times H_v$	--	--	--	--	-3.294(28)
γ_v	-0.05457(19)	-0.05463(19)	-0.05465(19)	0.16912(19)	0.24384(19)
$10^6 \times \gamma_{Dv}$	--	--	--	1.9726(98)	6.316(19)
$10^{10} \times \gamma_{Hv}$	--	--	--	0.4246(92)	3.484(26)

^aNumbers in parentheses are one standard deviation in last digit.

TABLE 5
Equilibrium Constants (in cm^{-1}) for ^{178}HfN and ^{180}HfN

Const. ^a	^{178}HfN		^{180}HfN	
	$X^2\Sigma^+$	$[6.7]^2\Sigma^+$	$X^2\Sigma^+$	$[6.7]^2\Sigma^+$
ω_e	933.0978(19)	$[969.9561(12)]^b$	932.7164(15)	$[969.57568(93)]^b$
$\omega_e x_e$	4.41741(86)	--	4.41299(65)	--
B_e	0.436585(15)	0.4192130(38)	0.436217(18)	0.4188611(26)
α_e	0.0026621(86)	0.0029392(45)	0.002659(11)	0.0029347(30)
r_e	1.724652(28)	1.7600229(80)	1.724678(36)	1.7600471(57)

^aNumbers in parentheses are one standard deviation in last digit.

^b $\Delta G(1/2)$ values.

thus corresponds to the analogous $A^1\Sigma^+ - X^1\Sigma^+$ infrared electronic transition of ScN (14) and YN (15). The ScN and YN transitions are between configurations that differ from those of HfN by the addition of a single nonbonding s electron on the metal.

The $A^2\Pi$ and $B^2\Sigma^+$ states result from the metal-centered promotion of the Hf $6s$ electron (3σ orbital) to the mainly Hf $6p\pi$ and $6p\sigma$ (2π and 4σ) orbitals. The $A^2\Pi$ and $B^2\Sigma^+$ states are a pure precession pair of states with large Λ -doubling in the regular $A^2\Pi$ state and a large negative spin-rotation constant in the $B^2\Sigma^+$ state. Presumably there is also a low-lying $^2\Delta$ state arising from the promotion of the Hf $6s$ electron to the Hf $5d\delta$ orbital. Additional low-lying states include a $^4\Delta$ state from the $(1\sigma)^2(1\pi)^4(2\sigma)^1(3\sigma)^1(1\delta)^1$ configuration and a $^2\Pi_i$ state from the $(1\sigma)^2(1\pi)^3(2\sigma)^2(3\sigma)^2$ configuration. Some ab initio calculations on the low-lying states of HfN would be most welcome.

The large positive γ constant for the $[6.7]^2\Sigma^+$ state suggests a strong interaction with a nearby $^2\Pi$ state. If the $[6.7]^2\Sigma^+$ state $[(1\sigma)^2(1\pi)^4(2\sigma)^1(3\sigma)^2]$ is modeled as a hole in a N $2p\sigma$ orbital then there should be an interaction with an inverted $^2\Pi$ state $[(1\sigma)^2(1\pi)^3(2\sigma)^2(3\sigma)^2]$ modeled as a hole in the N $2p\pi$ orbital. The pure precession relationship,

$$\gamma = 4AB/\Delta E_{\Pi-\Sigma},$$

predicts a $^2\Pi_i$ state about 1000 cm^{-1} below the $[6.7]^2\Sigma^+$ state using a value of -100 cm^{-1} for the spin-orbit constant, A .

The existence of a low-lying inverted $^2\Pi$ state below the $A^2\Pi_r$ state is also supported by the negative value of

γ in the ground states of TiN and ZrN and, presumably, HfN. Fletcher *et al.* (36) suggest that the configuration $(1\sigma)^2(1\pi)^3(2\sigma)^2(3\sigma)^1(1\delta)^1$ would provide a suitable $^2\Pi_i$ state for the interaction with the $X^2\Sigma^+$ state in TiN. Clearly more experimental and theoretical work is necessary to locate the missing low-lying states in TiN, ZrN, and HfN.

Although we are not completely confident about the assignment of the lower state of the $[6.7]^2\Sigma^+ - X^2\Sigma^+$ transition as the ground state of HfN, it is worthwhile to compare the spectroscopic constants with those of TiN and ZrN. The lower state equilibrium constants for ^{180}HfN are $\omega_e = 932.7164(15)\text{ cm}^{-1}$, $B_e = 0.436217(18)\text{ cm}^{-1}$, $\alpha_e = 0.002659(11)\text{ cm}^{-1}$, and $r_e = 1.724678(36)\text{ \AA}$ compared with the available data for the ground state of TiN (48), $\omega_e = 1049.28\text{ cm}^{-1}$, $B_0 = 0.6211\text{ cm}^{-1}$, and $r_0 = 1.5825\text{ \AA}$. The equilibrium vibrational constants for ZrN are not yet available but $B_0 = 0.4838\text{ cm}^{-1}$ and $r_0 = 1.6969\text{ \AA}$ (48). The comparison of the lower state molecular constants of HfN with those of HfO, TiN, and ZrN supports our assignments.

CONCLUSION

We have observed a $^2\Sigma^+ - ^2\Sigma^+$ transition of the previously unknown HfN molecule using a Fourier transform spectrometer. The bands observed in the $5500\text{--}6800\text{ cm}^{-1}$ region have been assigned to a $[6.7]^2\Sigma^+ - X^2\Sigma^+$ transition. A rotational analysis of the 0-0, 1-1, 0-1, and 1-2 bands has been carried out and molecular constants have been determined for the most abundant ^{178}HfN and ^{180}HfN isotopomers. The lower electronic state of HfN has an equilibrium bond length of $1.724678(36)\text{ \AA}$ and an equilibrium vibra-

tional frequency of $932.7164(15) \text{ cm}^{-1}$. More theoretical and experimental work on TiN, ZrN, and HfN is desirable to locate the missing low-lying electronic states and confirm our assignments in HfN.

ACKNOWLEDGMENTS

We thank J. Wagner, C. Plymate, and P. Hartmann of the National Solar Observatory for assistance in obtaining the spectra. The National Solar Observatory is operated by the Association of Universities for Research in Astronomy, Inc., under contract with the National Science Foundation. The research described here was supported by funding from the Petroleum Research Fund administered by the American Chemical Society and NASA laboratory astrophysics program. Support was also provided by the Natural Sciences and Engineering Research Council of Canada.

REFERENCES

1. C. W. Bauschlicher, Jr., S. P. Walch, and S. R. Langhoff, in "Quantum Chemistry: The Challenge of Transition Metals and Coordination Chemistry" (A. Veillard, Ed.), NATO ASI Ser. C. Reidel, Dordrecht, 1986.
2. S. R. Langhoff and C. W. Bauschlicher, Jr., *Ann. Rev. Phys. Chem.* **39**, 181–212 (1988).
3. M. Dolge, U. Wedig, H. Stoll, and H. Preuss, *J. Chem. Phys.* **86**, 2123–2131 (1987).
4. P. E. M. Siegbahn, *Chem. Phys. Lett.* **201**, 15–23 (1993).
5. C. J. Cheetham and R. F. Barrow, *Adv. High Temp. Chem.* **1**, 7–47 (1967).
6. M. Grunze, in "The Chemical Physics of Solid Surfaces and Heterogeneous Catalysis" (D. A. King and D. P. Woodruff, Eds.), Vol. 4, p. 143. Elsevier, New York, 1982.
7. F. A. Cotton and G. Wilkinson, "Advanced Inorganic Chemistry. A Comprehensive Text," 5th ed. Wiley, New York, 1988.
8. H. Machara and Y. Y. Yamashita, *Pub. Astron. Soc. Jpn* **28**, 135–140 (1976).
9. D. L. Lambert and R. E. S. Clegg, *Mon. Not. R. Astron. Soc.* **191**, 367–389 (1980).
10. Y. Yerle, *Astron. Astrophys.* **73**, 346–351 (1979).
11. B. Lindgren and G. Olofsson, *Astron. Astrophys.* **84**, 300–303 (1980).
12. D. L. Lambert and E. A. Mallia, *Mon. Not. R. Astron. Soc.* **151**, 437–447 (1971).
13. O. Engvold, H. Wöhl and J. W. Brault, *Astron. Astrophys. Suppl. Ser.* **42**, 209–213 (1980).
14. R. S. Ram and P. F. Bernath, *J. Chem. Phys.* **96**, 6344–6347 (1992).
15. R. S. Ram and P. F. Bernath, *J. Mol. Spectrosc.* **165**, 97–106 (1994).
16. R. S. Ram and P. F. Bernath, *J. Opt. Soc. Am. B* **11**, 225–230 (1994).
17. R. S. Ram, P. F. Bernath, W. J. Balfour, J. CaO, C. X. W. Qian, and S. J. Rixon, *J. Mol. Spectrosc.* **168**, 350–362 (1994).
18. W. J. Balfour, private communication.
19. E. J. Friedman-Hill and R. W. Field, *J. Chem. Phys.* **100**, 6141–6152 (1994).
20. K. Y. Jung, T. C. Steimle, D. Dai, and K. Balasubramanian, *J. Chem. Phys.* **102**, 644–652 (1995).
21. A. J. Marr, M. E. Flores, and T. C. Steimle, *J. Chem. Phys.* **104**, 8183–8196 (1996).
22. W. J. Balfour, C. X. W. Qian, and C. Zhou, *J. Chem. Phys.*, **106**, 4383–4388 (1997).
23. K. L. Kunze and J. F. Harrison, *J. Am. Chem. Soc.* **112**, 3812–3625 (1990).
24. I. Shim and K. A. Gingerich, *Int. J. Quant. Chem.* **46**, 145–157 (1993).
25. C. W. Bauschlicher, Jr., *Chem. Phys. Lett.* **100**, 515–518 (1983).
26. S. M. Mattar, Jr., *J. Phys. Chem.* **97**, 3171–3175 (1993).
27. J. F. Harrison, *J. Phys. Chem.* **100**, 3513–3519 (1996).
28. S. M. Mattar and B. J. Doleman, Jr., *J. Chem. Phys. Lett.* **216**, 369–374 (1993).
29. W. H. Parkinson and E. M. Reeves, *Can. J. Phys.* **41**, 702–704 (1963).
30. T. M. Dunn, L. K. Hanson, and K. A. Rubinson, *Can. J. Phys.* **48**, 1657–1663 (1970).
31. J. K. Bates, N. L. Ranieri, and T. M. Dunn, *Can. J. Phys.* **54**, 915–916 (1976).
32. C. Athénour, J.-L. Féménias, and T. M. Dunn, *Can. J. Phys.* **60**, 109–116 (1982).
33. A. E. Douglas and P. M. Veillette, *J. Chem. Phys.* **72**, 5378–5380 (1980).
34. K. Brabaharan, J. A. Coxon, and A. B. Yamashita, *Spectrochim. Acta A* **41**, 847–850 (1985).
35. K. Brabaharan, J. A. Coxon, and A. B. Yamashita, *Can. J. Phys.* **63**, 997–1004 (1985).
36. D. A. Fletcher, C. T. Scurlock, K. Y. Jung, and T. C. Steimle, *J. Chem. Phys.* **99**, 4288–4299 (1993).
37. J. K. Bates and T. M. Dunn, *Can. J. Phys.* **54**, 1216–1223 (1976).
38. J. K. Bates and D. M. Gruen, *High Temp. Sci.* **18**, 27–243 (1978).
39. H. Li, C. M.-T. Chan, and A. S.-C. Cheung, *J. Mol. Spectrosc.* **176**, 219–221 (1996).
40. C. M.-T. Chan, H. Li, N. S.-K. Sze, and A. S.-C. Cheung, *J. Mol. Spectrosc.* **180**, 145–149 (1996).
41. T. C. DeVore and T. N. Gallaher, *J. Chem. Phys.* **70**, 3497–3501 (1979).
42. G. Edvinsson and Ch. Nylén, *Phys. Scr.* **3**, 261–266 (1971).
43. R. S. Ram and P. F. Bernath, *J. Mol. Spectrosc.* **169**, 268–285 (1995).
44. B. A. Palmer and R. Engleman, "Atlas of the Thorium Spectrum." Los Alamos National Laboratory, Los Alamos, 1983.
45. J. Brown, E. A. Colbourn, J. K. G. Watson, and F. D. Wayne, *J. Mol. Spectrosc.* **74**, 294–318 (1979).
46. M. Douay, S. A. Rogers, and P. F. Bernath, *Mol. Phys.* **64**, 425–436 (1988).
47. G. Herzberg, "Molecular Spectra and Molecular Structure I. Spectra of Diatomic Molecules." Van Nostrand-Reinhold, New York, 1950.
48. K. P. Huber and G. Herzberg, "Molecular Spectra and Molecular Structure IV. Constants of Diatomic Molecules." Van Nostrand-Reinhold, New York, 1979.